Modified Soft-Switching System With Safe Connections of Capacitors and Inductors in Three-Phase Voltage Source Inverter

Witold Mazgaj and Zbigniew Szular

***Abstract*—This article presents a modified soft-switching system for three-phase voltage source inverters. Similar to the basic soft-switching system, capacitors are not connected in parallel to the main transistors, and inductors are not connected in series with the auxiliary transistors. These connections protect the inverter from damage when disturbances occur in the control system. Unlike the basic version, the modified soft-switching system does not allow resonant processes to affect the voltage waveform on the load, and the modified system features a simpler control algorithm for the main and auxiliary transistors. The structure and operating principles of the modified soft-switching solution are comprehensively described herein. Additionally, the principles for selecting the elements of the modified soft-switching system are discussed. The system's operation is validated through laboratory tests using a three-phase voltage source inverter (10 kW, 400 V) to supply a squirrel-cage induction motor, whereas numerical calculations are performed for inverters with higher rated power. The switching losses of the inverter operating under the modified soft-switching solution are compared with those of an inverter operating under the hard-switching technique. Results show that the proposed modified soft-switching system increases inverter efficiency .**

***Index Terms*—Soft switching, switching losses, voltage source inverter, ZCZVS converter.**

I. Introduction

THE efficiency of voltage source inverters (VSIs) depends on the power losses that occur in insulated-gate bipolar transistors (IGBTs) and their freewheeling diodes. These losses are the sum of conduction and switching losses [1], [2], [3], [4]. Conduction losses depend on the current and voltage drops across a specified transistor or diode during conduction. Switching losses are caused by simultaneous changes in the transistor voltage and current during turn-ON or turn-OFF processes. VSI users cannot affect conduction losses; however, they can reduce switching losses using soft-switching systems, which cause the transistor current or voltage to approach zero during the switching processes. In soft-switching systems, circuits containing auxiliary transistors, capacitors, and inductors are incorporated into the structure of a typical two-level VSI. This allows the voltage or current of the main transistors to gradually increase from zero during the switching process. Converters with such properties are called ZCZVS converters.

In some proposed methods, the same one or two soft-switching circuits support the switching processes in all inverter phases [5], [6], [7], [8], [9], [10], [11], [12], thus reducing the number of additional elements. However, the control algorithms of these systems are typically complex, and the frequency of the inverter output voltage can change within a narrow range. In these cases, the resonant processes associated with switching the transistors in any inverter phase affect the output voltages of the remaining phases.

In most solutions, each phase of a three-phase VSI comprises individual soft-switching circuits with additional transistors and passive elements [13], [14], [15], [16], [17], [18], [19], [20], [21], [22]. In many soft-switching systems, a sudden capacitor discharge may occur in the case of disturbances, especially if the capacitors are connected in parallel to the main transistors [15], [16], [17], [19], [20], [21], [22], [23]. In some proposals, inductors are connected in series with auxiliary transistors. When one of these transistors is turned OFF while the current of the inductor is nonzero, it can result in an overvoltage [14], [17]. The soft-switching system presented in [13] lacks parallel connections between the main transistors and capacitors, as well as series connections between the inductors and auxiliary transistors. However, its control algorithm is complex because the switching processes of the main transistors depend on the operating states of the auxiliary transistors.

Issues related to soft-switching are also relevant to VSIs constructed using SiC MOSFETs. Even though the switching frequencies are much higher than those in inverters with IGBTs, the problem of reducing switching losses has qualitatively the same character. Proposals for VSIs with SiC MOSFETs involve the use of resonant circuits with additional controlled switches [24], [25], [26], [27], [28].

The main disadvantages of the soft-switching systems proposed thus far are the risk of sudden capacitor discharge and complex control algorithms. Often, the control signals for auxiliary transistors must be generated before switching the main transistors. A soft-switching system with safe connections between the capacitors and inductors in a three-phase two-level VSI was proposed in [29] and [30], and its structure is shown

Received 19 April 2024; revised 5 July 2024 and 12 August 2024; accepted 21 September 2024. Date of publication 2 October 2024; date of current version 12 December 2024. This work was supported by the Polish Ministry of Science and Higher Education and performed by the Department of Electrical Engineering of Cracow University of Technology. Recommended for publication by Associate Editor J. He. *(Corresponding author: Zbigniew Szular.)*

The authors are with the Department of Electrical Engineering, Cracow University of Technology, 31-155 Krakow, Poland (e-mail: pemazgaj@cyfronet.pl; zbigniew.szular@pk.edu.pl).

Color versions of one or more figures in this article are available at https://doi.org/10.1109/TPEL.2024.3472223.

Digital Object Identifier 10.1109/TPEL.2024.3472223

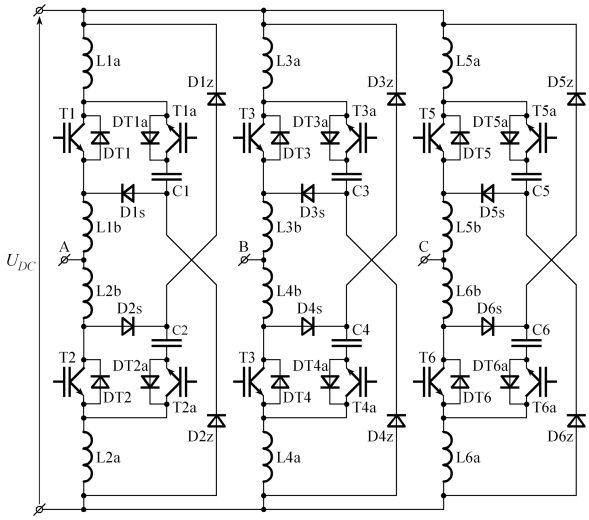

Fig. 1. Basic soft-switching system with safe connections of capacitors and inductors in three-phase inverter [30].

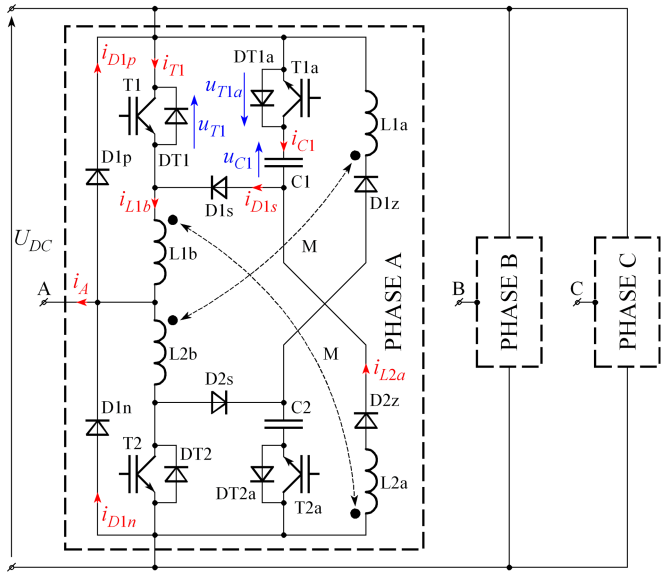

Fig. 2. One phase of a modified soft-switching system with safe connections of capacitors and inductors in a three-phase inverter; M represents a magnetic coupling.

in Fig. 1. In this soft-switching system, the capacitors are not connected in parallel to the main transistors, and the inductors are not connected in series with the auxiliary transistors. This configuration prevents the discharging of capacitors through the main transistors and abrupt interruptions of the inductor currents, thus enhancing the reliability of the VSIs operating under the proposed soft-switching system. However, in the system presented in [30], the resonance processes associated with soft-switching affect the shape of the load voltage. Additionally, the control signals of the auxiliary transistors depend on those of the main transistors, as they are turned ON with a certain delay relative to the main transistors.

The following sections describe the operating principles of the modified soft-switching system, which eliminates the risk of sudden capacitor discharge and features a simpler control algorithm compared to the basic system [30]. The inductors are connected differently to the transistors, with negative magnetic coupling applied between the appropriate inductors. Due to this modification, the resonant processes do not affect the load voltage, significantly simplifying the inverter control system.

Soft-switching systems without additional auxiliary transistors were proposed in [31] and [32]. The proposal described in [31] refers to a single-phase low-power inverter in wireless power transfer systems. A passive soft-switching system applied in a three-phase VSI was described in [32]. However, the authors assumed that in several working stages, the currents of the additional inductors flowed through the diodes, and the energy of the magnetic field of these inductors was dissipated in the diodes.

II. Modified Soft-Switching System With Safe Connections of Capacitors and Inductors

A. Structure and Operation Principles

The modified soft-switching solution (see Fig. 2), initially proposed in [33], does not feature the aforementioned disadvantages of existing soft-switching systems, and its operation does not affect the voltage waveforms of the load.

The capacitors should reduce the steepness of the voltage increase in the main transistors during the turn-OFF processes. The inductors connecting the main transistors to the load terminals should limit the rate of current increase in these transistors during their turn-ON processes. The inductors connected in series with the diodes should limit the resonant discharge current of the capacitors. Additionally, the negative magnetic coupling between the inductors must be prioritized. This coupling helps to reduce the current of the inductors connected to the transistors to zero after they are turned OFF. When the currents of these inductors are significantly greater than zero, turning ON the main transistors becomes a hard switching, as will be described in detail later in this section.

B. Operating Stages

The operation of the modified soft-switching system is described for one switching cycle, with the assumption that the load current I_A remains constant in all considered states. Simplified waveforms of the selected voltages and currents are shown in Fig. 3.

The analysis was performed for cases where transistor T1 was switched, transistor T2 was in a nonconducting state, and capacitor C1 was discharged. The circuit with current is indicated by the bold red line in Fig. 4(a).

Stage t_1–t_2: As shown in Fig. 4(b), transistor T1 is turned OFF at time t_1 and its voltage increases gradually from zero due to the charging of capacitor C1. The voltage of the main transistor T1 changes in the same manner as the voltage of capacitor C1 because, in this stage, the load current I_A flows through diode DT1a, capacitor C1, diode D1s, and inductor L1b. Therefore, the main transistor T1 is turned OFF softly. The voltage across

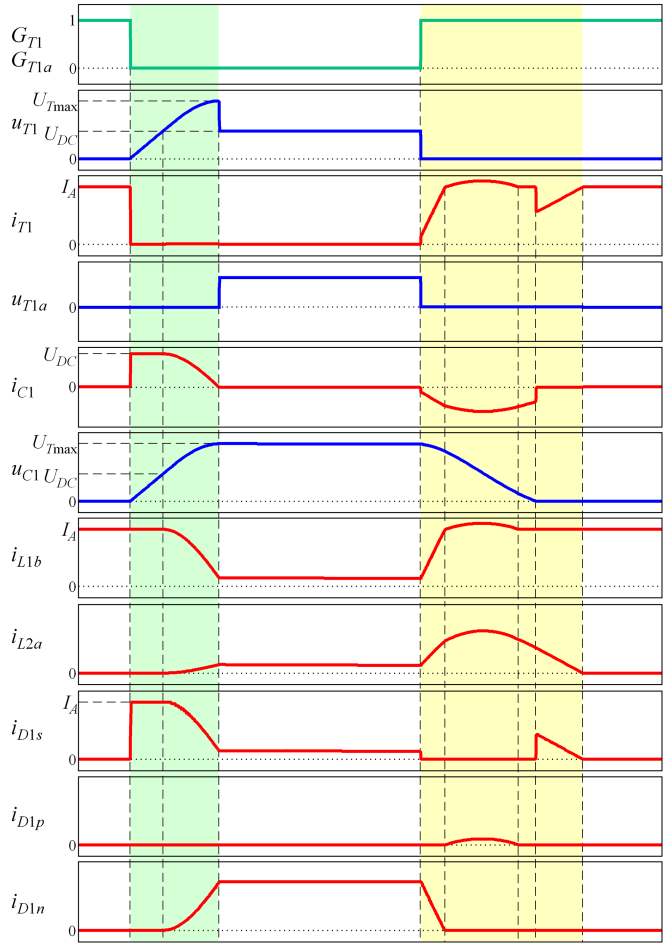

Fig. 3. Simplified waveforms in one phase of modified soft-switching solution: G_{T1} and G_{T1a}: control signals of transistors T1 and T1a, respectively; i_{T1} and u_{T1}: current and voltage of transistor T1, respectively; u_{T1a}: voltage of transistor T1a; i_{C1} and u_{C1}: current and voltage of capacitor C1, respectively; i_{L1b} and i_{L2a}: currents of inductors L1b and L2a, respectively; i_{D1s}, i_{D1p}, and i_{D1n}: currents of diodes D1s, D1p, and D1n, respectively; I_A: load current, and period t_1–t_3: processes related to soft turning OFF of transistor T1 and period t_4–t_8: processes related to soft turning ON of transistor T1.

capacitor C1 increases linearly with time

$$u_{C1}(t) = \frac{I_A(n)}{C_1}\, t \tag{1}$$

where $u_{C1}(t_1) = 0$, n is the number of switching cycles, and $I_A(n)$ is the load current in the nth switching cycle. This operating stage continues until the voltage of capacitor C1 reaches supply voltage U_{DC}. The duration of this process depends on the load current I_A.

Stage t_2–t_3: As shown in Fig. 4(c), at time t_2, the voltage of capacitor C1 reaches supply voltage U_{DC}. At this point, diodes D1n and D2z begin to conduct. The current through inductor L1b is the sum of the currents flowing through capacitor C1 and diode D2z, which is connected in series with inductor L2a. Simultaneously, the current through the capacitor decreases. The capacitor is charged to a voltage higher than U_{DC}, and the changes in the capacitor voltage are expressed as

$$\begin{cases} u_{C1} + L_{1b}\frac{di_{L1b}}{dt} - M\frac{di_{L2a}}{dt} = U_{\mathrm{DC}} \\ L_{1b}\frac{di_{L1b}}{dt} - M\frac{di_{L2a}}{dt} + L_{2a}\frac{di_{L2a}}{dt} - M\frac{di_{L1b}}{dt} = 0 \\ i_{L1b} - i_{C1} - i_{L2a} = 0 \end{cases} \tag{2}$$

where $u_{C1}(t_2) = U_{\mathrm{DC}}$, $i_{L1b}(t_2) = I_A(n)$, $i_{L2b}(t_2) = 0$, and M is the mutual inductance of negative magnetic coupling.

Inductors L1a and L2a have the same inductance L_a, the inductances of inductors L1b and L2b are L_b, and capacitors C1 and C2 have the same capacitance C. Equation (2) can be replaced with a differential equation as follows:

$$CL_r\frac{d^2u_c}{dt^2} + u_C = U_{\mathrm{DC}} \tag{3}$$

where

$$L_r = \frac{L_aL_b - M^2}{L_a - 2M + L_b}. \tag{4}$$

The changes in the voltage and current of capacitor C1 at this stage are expressed as follows:

$$u_{C1}(t) = U_{\mathrm{DC}} + \sqrt{\frac{L_r}{C}}I_A(n)\sin\left(\frac{t}{\sqrt{CL_r}}\right) \tag{5}$$

$$i_{C1}(t) = I_A(n)\cos\left(\frac{t}{\sqrt{CL_r}}\right). \tag{6}$$

The maximum voltage of capacitor C1 in the specified switching cycle is expressed as

$$U_{C1\,\max}(n) = U_{DC} + \sqrt{\frac{L_r}{C}}I_A(n). \tag{7}$$

In the time interval t_1–t_3, the voltage of the main transistor T1 changes with the voltage of capacitor C1. At time t_3, both voltages reach their highest values in the analyzed switching cycle.

As mentioned earlier, the current through inductor L1b should decrease to zero to ensure that the next turn-ON process of transistor T1 is soft. During this operational stage, any current in inductor L2a is undesirable because it causes current to flow from the negative clamp of the voltage source through inductor L2a, diodes D2z and D1s, and inductor L1b. If the current in inductor L1b decreases, a voltage is induced in inductor L2a that opposes the current flowing through it. The magnitude of this voltage depends on the mutual inductance M. When T1 is turned OFF, the entire load current flows through diode D1n. The currents in inductors L1b and L2a are reduced by employing an appropriately selected negative magnetic coupling M.

The current in inductor L1b should be zero after the turn-OFF processes for transistor T1 are completed. However, this approach can cause a current to appear in diode D1p during the resonant discharge of capacitor C1 when transistor T1 is turned ON again [see Fig. 4(f)]. At the end of this time interval, the currents in inductors L1b and L2a are expressed as

$$i_{L1b}(t_3) = i_{L2a}(t_3)$$

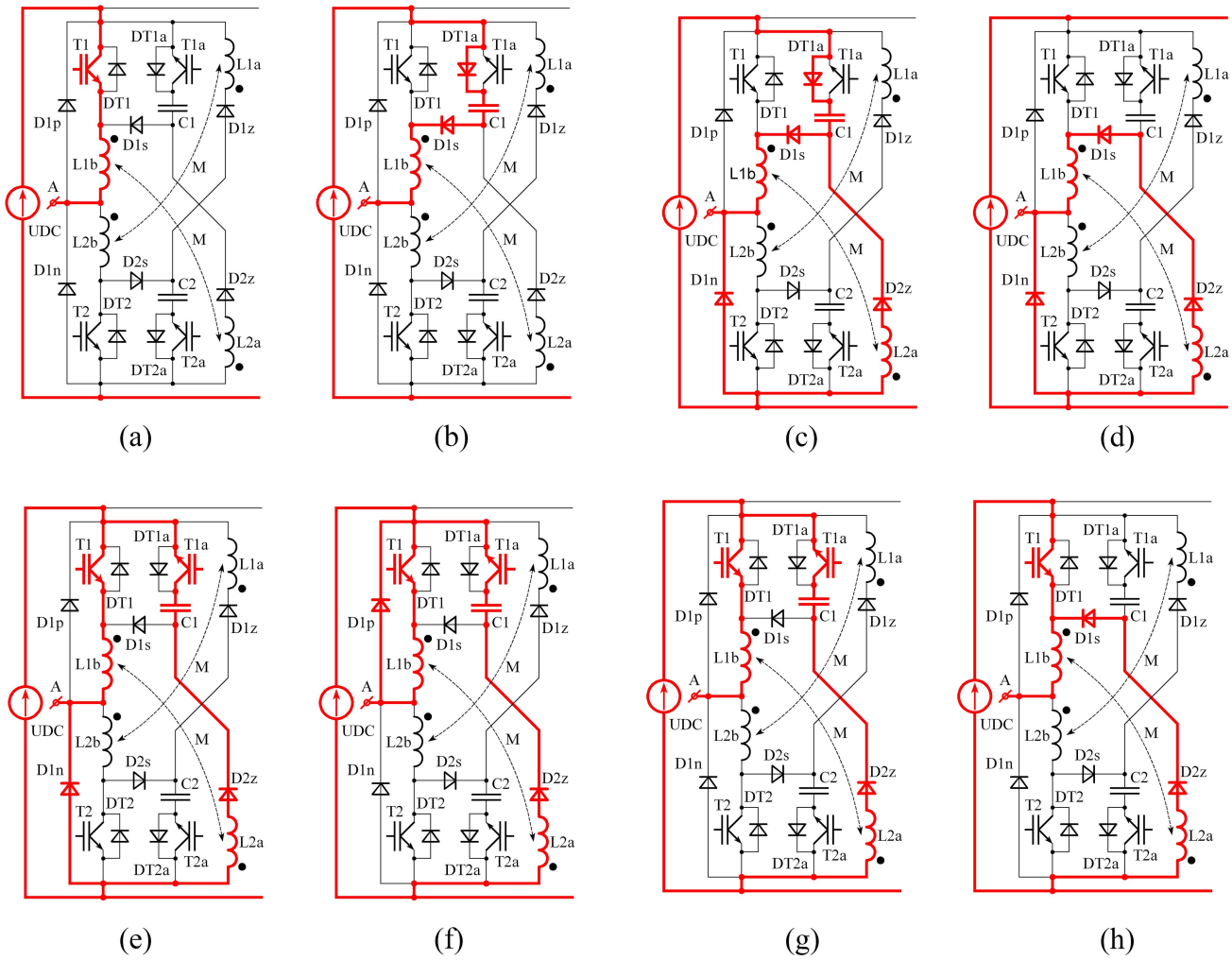

Fig. 4. Operation stages of the modified soft-switching system. (a) Before T1 is turned OFF; (b) t_1–t_2; (c) t_2–t_3; (d) t_3–t_4; (e) t_4–t_5; (f) t_5–t_6; (g) t_6–t_7; (h) t_7–t_8.

$$= \frac{L_b - M}{L_a - 2M + L_b} I_A(n) \left(1 - \cos \frac{t_3}{\sqrt{CL_r}}\right). \tag{8}$$

To ensure a soft subsequent turn-ON process for transistor T1, the current through inductor L1b should be zero after the turn-OFF process for this transistor is completed. This implies that the mutual inductance M should be equal to the inductance L_b.

Stage t_3–t_4: At time t_3, the currents through capacitors C1 and diode DT1a are zero. Since then, diode DT1a has been reverse-biased, and it changes its operating state without losses. The voltage of capacitor C1 remains unchanged, whereas the voltage of transistor T1 decreases rapidly to the supply voltage U_{DC}. The load current I_A primarily flows from the negative clamp of the voltage source through diode D1n [see Fig. 4(d)]. A relatively small current flows through inductor L2a, diode D2z, and inductor L1b. This current reaches a certain value at time t_3. During this interval, transistor T1 is in a nonconducting state, and the voltages of the individual elements in the inverter phase remain unchanged.

Stage t_4–t_5: As shown in Fig. 4(e), at time t_4, the main transistor T1 and auxiliary transistor T1a are turned ON, and diode D1s stops conducting. The turn-OFF losses of the diode can be neglected because it changes its operating state at a relatively low current. The currents in transistors T1 and L1b begin to gradually increase to the load current I_A, whereas the current through diode D1n decreases to zero. The main transistor T1 is turned ON with a current close to zero, ensuring a soft turn-ON process. Simultaneously, capacitor C1 begins to discharge. Changes in the current and capacitor voltage are described by the following equations, assuming $i_{L2a} = -i_{C1}$:

$$\begin{cases} L_{1b} \frac{di_{L1b}}{dt} + M \frac{di_{C1}}{dt} = U_{\mathrm{DC}} \\ u_{C1} + L_{2a} \frac{di_{C1}}{dt} + M \frac{di_{L1b}}{dt} = U_{\mathrm{DC}} \end{cases} \tag{9}$$

where $i_{L1b}(t_4)$ is the constant current flowing in inductor L1b in stage t_3–t_4, and $u_{C1}(t_4)$ denotes the maximum voltage of capacitor C1 (7).

Assuming that the mutual inductance M is similar to the inductance L_b and that the current through inductor L1b is small relative to the load current I_A, the changes in the capacitor

voltage and current can be expressed as

$$u_{C1}(t) = U_{C\max}\cos\left(\frac{t}{\sqrt{C(L_a - L_b)}}\right) \tag{10}$$

$$i_{C1}(t) = -\sqrt{\frac{C_1}{L_a - L_b}}U_{C\max}\sin\left(\frac{t}{\sqrt{C(L_a - L_b)}}\right). \tag{11}$$

A negative sign indicates that the current flows in the direction opposite to that shown in Fig. 2. Notably, if $M = L_b$, the changes in the capacitor voltage and current do not depend on the source voltage U_{DC}. The changes in the current through inductor L1b can be expressed as

$$i_{Lb1}(t) = \frac{U_{\mathrm{DC}}}{L_b}t + \sqrt{\frac{C_1}{L_a - L_b}}U_{C\max}\sin\left(\frac{t}{\sqrt{C(L_a - L_b)}}\right). \tag{12}$$

At time t_5, this current reaches the load current value I_A.

Stage t_5–t_6: At time t_5, diode D1n stops conducting. This diode changes its operating state without losses because its current gradually decreases to zero during the interval t_4–t_5. During the period t_5-t_6, capacitor C1 continues to discharge [see Fig. 4(f)]. Due to the magnetic coupling between inductors L1b and L2a, a small current appears in circuits T1, L1b, and D1p, which decreases to zero at time t_6. The changes in the current and capacitor voltage are expressed as follows, assuming $i_{L2a} = -i_{C1}$:

$$\begin{cases} L_{1b}\frac{di_{L1b}}{dt} + M\frac{di_{C1}}{dt} = 0 \\ u_{c1} + L_{2a}\frac{di_{C1}}{dt} + M\frac{di_{L1b}}{dt} = U_{\mathrm{DC}} \end{cases} \tag{13}$$

where $i_{L1b}(t_5) = 0$ because the load current flowing through inductor L1b is constant in the considered operational cycle. The changes in $u_{C1}(t_5)$ and $i_{C1}(t_5)$ were determined using (10) and (11), respectively.

The capacitor voltage and current as well as the current of inductor L1b change as

$$\begin{aligned} u_{C1}(t) = {} & u_{C1}(t_5)\cos\left(\frac{t}{\sqrt{C(L_a - L_b)}}\right) \\ & + i_{L2a}(t_5)\sqrt{\frac{L_a - L_b}{C}}\sin\left(\frac{t}{\sqrt{C(L_a - L_b)}}\right) \\ & + U_{DC}\left(1 - \cos\frac{t}{\sqrt{C(L_a - L_b)}}\right) \end{aligned} \tag{14}$$

$$\begin{aligned} i_{C1}(t) = {} & i_{L2a}(t_5)\cos\left(\frac{t}{\sqrt{C(L_a - L_b)}}\right) \\ & - \sqrt{\frac{C_1}{L_a - L_b}}(u_{C1}(t_5) - U_{\mathrm{DC}})\sin\left(\frac{t}{\sqrt{C(L_a - L_b)}}\right) \end{aligned} \tag{15}$$

$$\begin{aligned} i_{L1b}(t) = {} & I_A + i_{L2a}(t_5)\left(1 - \cos\frac{t}{\sqrt{C(L_a - L_b)}}\right) \\ & + \sqrt{\frac{C_1}{L_a - L_b}}(u_{C1}(t_5) - U_{\mathrm{DC}})\sin\left(\frac{t}{\sqrt{C(L_a - L_b)}}\right). \end{aligned} \tag{16}$$

The maximum current value of inductor L1b must be determined, as it allows for the calculation of the maximum current values for diode D1p and transistor T1. Therefore, the moment $t_{L1b\max}$, when the current through inductor L1b reaches its maximum, must be determined as

$$t_{L1b\max} = \sqrt{C(L_a - L_b)} \arcsin\left(\sqrt{1 + \frac{L_a - L_b}{C}\left(\frac{i_{L2a}(t_5)}{u_{C1}(t_5) - U_{\mathrm{DC}}}\right)^2}\right)^{-1}. \tag{17}$$

By introducing time $t_{L1b\max}$ into (16), the maximum current of inductor L1b can be determined. The current flowing through diode D1p is the difference between the current through inductor L1b and the load current I_A.

Stage t_6–t_7: At time t_6, the current through diode D1p decreases to zero. Only the load current I_A flows through transistor T1, whereas capacitor C1 continues to discharge [see Fig. 4(g)].

Stage t_7–t_8: At time t_7, the voltage of capacitor C1 drops to zero, causing auxiliary transistor T1a to turn-OFF with zero current. During this interval, the current through inductor L2a flows through diode D1s and decreases to zero at time t_8 [see Fig. 4(h)].

The energy stored in capacitor C1 is returned to the voltage source during the time interval t_4-t_8. At low load currents, the maximum voltage of capacitor C1 may be less than twice the supply voltage. Consequently, the capacitor is not fully discharged, and the subsequent turn-OFF of T1 is not soft. Capacitor C1 is fully discharged only if its maximum voltage is at least twice the supply voltage U_{DC}.

C. Switching Algorithm

In the modified soft-switching system, the auxiliary and main transistors are turned ON simultaneously, in contrast to the basic soft-switching system [30], where the control signals for the auxiliary transistors are delayed relative to those for the main transistors. This simultaneous switching simplifies the control system, which is beneficial for pulsewidth modulation (PWM) applications in the VSI. However, appropriate time intervals for the soft-switching processes must be accounted for when determining the maximum modulation depth factor for a given switching frequency.

As in traditional VSIs, the main transistors can be controlled using a hard-switching technique. However, after turning OFF T1 and turning ON T2, a relatively small current flows through inductor L2b and transistor T2, respectively. When T2 is turned OFF again, the current of inductor L2b flows through diode D2s, capacitor C2, and diode DT2a, causing a slight increase in the voltage of capacitor C2. Numerical calculations indicate that the losses due to these currents do not exceed 0.2% of the total losses in the inverter with the proposed soft-switching system.

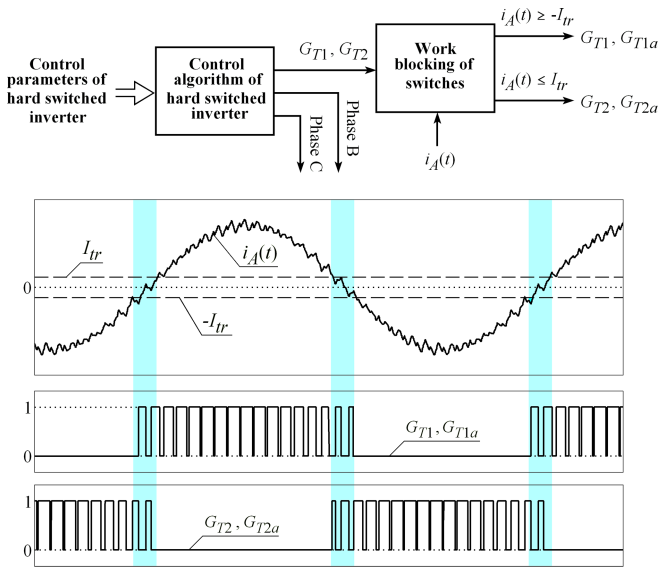

Fig. 5. Generation of control signals of transistors; marked periods—time intervals in which both main transistors T1 and T2 are switched.

To eliminate these losses, an alternative control method for transistors T1 and T2 in the considered phase has been proposed.

In the analysis of inverter operation, transistor T2 is assumed to be in a nonconducting state when T1 is switched. The instantaneous load current $i_A(t)$ should be compared with the threshold currents, $-I_{\rm tr}$ and $+I_{\rm tr}$ (see Fig. 5). When the load current exceeds $+I_{\rm tr}$, the main transistor T1 is switched, and T2 is in the nonconducting state. When this current is lower than the value $-I_{\rm tr}$, transistor T2 is switched and T1 is in a nonconducting state. In the case when the instantaneous value $i_A(t)$ of the load current ranges between $-I_{\rm tr}$ and $+I_{\rm tr}$, both transistors are turned ON and OFF. The main transistors and the corresponding auxiliary transistors are controlled by the same control signal, which significantly simplifies the control algorithm.

III. Selection of Soft-Switching Elements

A. Selection of Transistors

Due to resonant processes, transistors should be rated for voltages higher than the supply voltage $U_{\rm DC}$. After the main transistors are turned OFF, the capacitors charge to a voltage exceeding $U_{\rm DC}$ which appears across the main transistors once resonant charging is completed.

To ensure a soft turn-OFF process for the main transistors, the maximum capacitor voltage should be at least twice $U_{\rm DC}$. Although selecting transistors rated for this maximum voltage may be inconvenient, the proposed soft-switching system mitigates overvoltage risk for the main transistors, as each transistor is paired with its own capacitor through a diode.

The main transistors must be rated for the maximum load current and the relatively small current present during the interval t_5–t_6 in circuits T1, L1b, and D1p [see Fig. 4(f)]. The maximum current for the auxiliary transistors depends on the peak discharge current of the capacitors. However, these transistors operate for much shorter durations than the main transistors, resulting in significantly lower conduction losses. The presence of inductors helps prevent sudden current surges in both main and auxiliary transistors, and they also limit the rate of current increase in the event of simultaneous turn-ON of both main transistors in any phase.

B. Reactive Elements

The primary function of the capacitors is to mitigate the rapid increase in the main transistor's voltage during the turn-OFF process. After the main transistor T1 is turned OFF, its current decreases quickly to zero. Similar to the voltage behavior of capacitor C1, the voltage across transistor T1 gradually rises from zero. If this voltage, following the completion of the turn-OFF process, does not exceed the specified value $U_{C\rm off}$ (which is a few percent or up to a dozen percent of $U_{\rm DC}$), then based on (1), the capacitance C can be determined using

$$C \geq \frac{I_{A\max}}{U_{C\rm off}} t_f \tag{18}$$

where $I_{A\max}$ denotes the maximum load current, and t_f is the time interval during which the main transistor's current decreases from 90% to 10% of its maximum value.

For the main transistor to be turned OFF softly, the corresponding capacitor must be fully discharged before the transistor is switched OFF. This condition is met if the maximum capacitor voltage is at least twice $U_{\rm DC}$. This is a key requirement for the proper functioning of the soft-switching system. Based on (7) and assuming that the maximum capacitor voltage is $k_{\max}U_{\rm DC}$ and $M = L_b$, the inductance L_b can be expressed as

$$L_b = C\left[\frac{(k_{\max}-1)U_{\rm DC}}{I_{A\max}}\right]^2 \tag{19}$$

where $k_{\max}$ is the ratio of the maximum capacitor voltage to the supply voltage $U_{\rm DC}$.

The primary role of inductors Lb1 and Lb2 is to mitigate the rapid increase in current through the main transistors after they are turned ON. Inductors L1a and L2a serve functions similar to those of the auxiliary transistors. The turn-ON process is considered soft switching if the transistor current during the time period t_r is approximately zero, where t_r denotes the time between when the main transistor current rises from 10% to its maximum value and when the main transistor voltage drops to 10% of its maximum value. The inductance L_a cannot be analytically determined using (11) and (12). Given that the transistor current rise time t_r, as specified in datasheets, is relatively short compared to the denominator $\sqrt{C(L_a - L_b)}$, the sine function in (11) and (12) can be approximated by its argument. The error between the exact and approximate values is less than 0.5%. Therefore, formula (11) for time t_r can be expressed as

$$i_{C1}(t_r) \approx -\frac{k_{\max}U_{\rm DC}}{L_a - L_b} t_r. \tag{20}$$

In stage t_4–t_5, the current through inductor L2a is equal in magnitude but opposite in direction to the current through capacitor C1. Assuming that the current through transistor T1a at time t_r does not exceed $I_{T\rm on}$ (a few or several percent of the

TABLE I
PARAMETERS OF TYPE-SKM100GB176D IGBT

V_{CC} (V)	I_C (A)	t_{on} (ns)	t_r (ns)	t_{off} (ns)	t_f (ns)	I_{rrm} (A)	V_{CE} (V)
1700	90.0	280	40	680	140	78.5	2.4

transistor's maximum current), the inductance L_a should satisfy the following condition ($i_{L2a} = -i_{C1}$):

$$L_a \geq \frac{k_{\max} U_{\mathrm{DC}}}{I_{T\mathrm{on}}} t_r + L_b. \tag{21}$$

Under the same assumption regarding the simplification of the sine function, formula (12) expressing the current of inductor L1b can be written as

$$i_{Lb1}(t_r) \approx \frac{U_{\mathrm{DC}}}{L_b} t_r + \frac{k_{\max} U_{\mathrm{DC}}}{L_a - L_b}. \tag{22}$$

Based on the previous relationship, the second condition for inductance L_a is as

$$L_a \geq \frac{k_{\max} U_{\mathrm{DC}}}{\frac{I_{T\mathrm{on}}}{t_r} - \frac{U_{\mathrm{DC}}}{L_b}} + L_b. \tag{23}$$

The maximum current flowing through diode D1p during the interval t_5–t_6 depends on the inductances L_a, L_b, and the mutual inductance M. While reducing the mutual inductance M may lower this maximum current, some current will still appear in inductors L1b and L2a during the nonconducting period of transistor T1.

The inductance and capacitance of the reactive elements are influenced by both the maximum load current $I_{A\max}$ and the coefficient $k_{\max}$. It is also crucial to determine the maximum voltage $U_{C\mathrm{off}}$ during the transistor turn-OFF process and the maximum value $I_{T\mathrm{on}}$ at which the transistor current can increase during the turn-ON process.

In the interval t_3–t_4, the current through inductor L1b is zero if the mutual inductance M equals the inductance L_b. However, in the interval t_5–t_6, a low current flows through diode D1p. To reduce this current, the value of M must be determined. Consequently, in the interval t_3–t_4, a relatively low current flows through inductor L1b, compared to the load current. The effects of varying mutual inductance M are discussed in Section V-A.

IV. LABORATORY INVESTIGATION

To verify the functionality of the modified soft-switching method, a three-phase laboratory VSI with a rated power of 10 kW was constructed. It utilized an IGBT-type SKM100GB176D (see Table I) and a diode-type DSEP30-12A (1200 V, 30 A, forward voltage 2.15 V). The IGBTs and their drivers, capacitors, current transducers, and overcurrent protection circuits were mounted on a steel plate [see Fig. 6(a)]. The inductors were placed on the opposite side of the plate to minimize their magnetic field's impact on the control circuits. Fig. 6(b) illustrates the control system.

The inverter was supplied with a voltage of 400 V, and the permissible load current was 12 A. Measurements were conducted using a laboratory inverter with a squirrel-cage induction

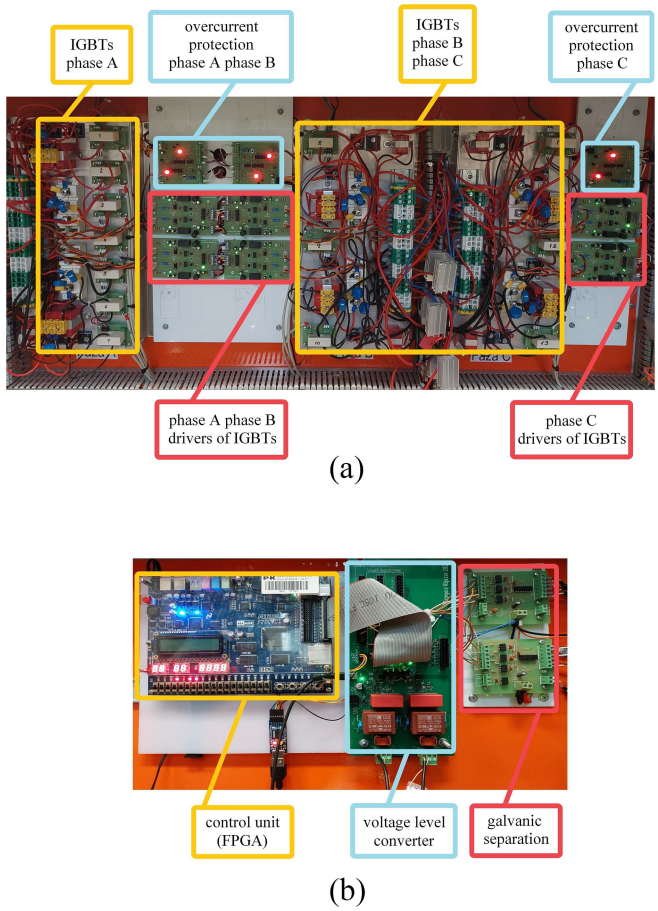

Fig. 6. Laboratory prototype of inverter with modified soft-switching system. (a) Power circuits. (b) Control system.

motor ($P_N = 3$ kW, $U_N = 230/400$ V Δ/Y). To qualify the switching processes as soft, it was assumed that the transistor current during the turn-ON processes could not exceed 10% of the maximum load current, and the transistor voltage during the turn-OFF processes could not exceed 10% of the supply voltage U_{DC}. The laboratory VSI with the modified soft-switching system utilized capacitors and inductors with greater capacities and inductances than those specified in the previous section. In this study, the laboratory investigations were performed with the following parameters: $C = 0.5$ μF, $L_a = 332$ μH, and $L_b = 127$ μH.

Fig. 7 shows the current and voltage waveforms of transistors T1 and T1a, with green and yellow colors representing the processes related to the soft turn-OFF and soft turn-ON of transistor T1, respectively. As transistor T1 is turned OFF, capacitor C1 begins charging, and its voltage increases gradually from zero, with the transistor voltage following a similar pattern. After transistor T1 is turned ON, its voltage immediately decreases to zero, whereas its current gradually increases from zero.

Simultaneously, transistor T1a is turned ON, and the resonant capacitor begins discharging. Fig. 8 shows the current waveforms of transistor T1, inductors L1b and L2a, and diode D1n for the same switching cycles. During the nonconduction interval of transistor T1, a small current of approximately 0.4 A flowed

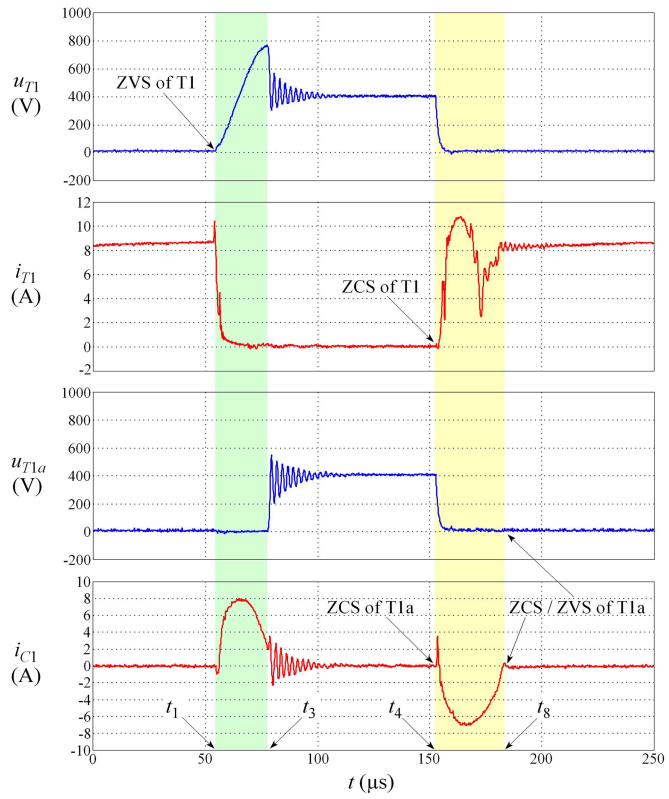

Fig. 7. Waveforms in one switching cycle: u_{T1} and i_{T1}—voltage and current of transistor T1, respectively; $u_{T1\,a}$ and $i_{T1\,a}$—voltage and current of transistor T1a and its freewheeling diode, respectively; $U_{\mathrm{DC}} = 400$ V, output frequency 40 Hz, switching frequency 2.4 kHz, modulation depth factor 0.85, $C = 0.5$ μF, $L_a = 332$ μH, and $L_b = 127$ μH, period t_1–t_3: processes related to soft turning OFF of transistor T1, and period t_4–t_8: processes related to soft turning ON of transistor T1 and soft turning ON and turning OFF of auxiliary transistor T1a.

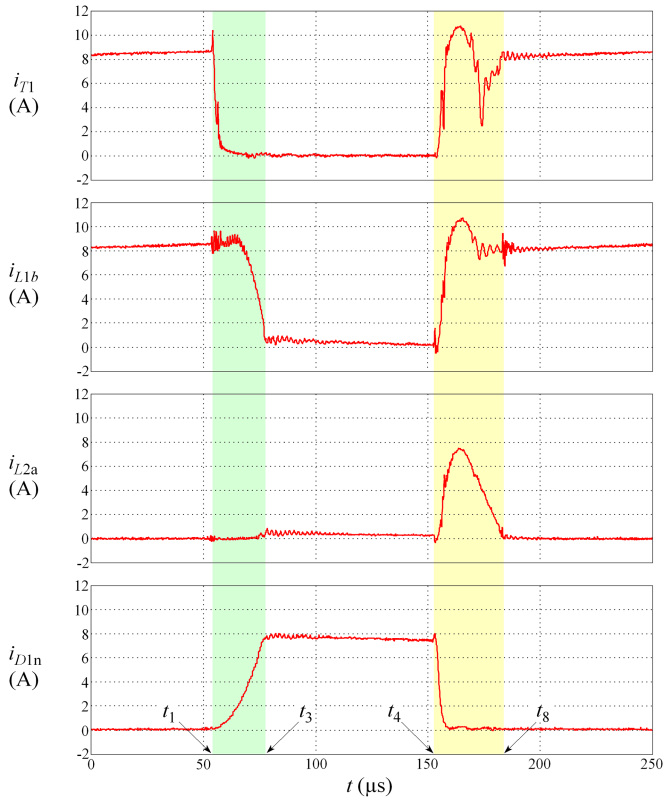

Fig. 8. Waveforms in one switching cycle: i_{T1}—current of transistor T1; $i_{L1\,b}$ and $i_{L2\,a}$—currents of inductor L1b and L2a, respectively; and $i_{D1\,n}$—current of diode D1n; and operating parameters are the same as those for Fig. 7.

through inductors L1b and L2a, as the mutual inductance M of the negative magnetic coupling between inductors L1b and L2a was not exactly equal to the inductance L_b.

The prototype inverter with the modified soft-switching system was equipped with air-core inductors to ensure their constant inductance regardless of the current. In industrial applications, these inductors are typically manufactured using ferrite cores with an air gap due to the high resistivity of ferrites. The dimensions of the inductors and losses in the windings depend on the core shape, air gap, and the magnetic induction in the ferrite core, which is usually no higher than approximately 0.3 T. Numerical calculations performed using finite element method magnetics software indicated that, due to the smaller number of turns in inductors with ferrite cores, losses in the inductor windings maybe three to five times lower than those in air-core inductors. It is also worth noting that hysteresis losses account for approximately a dozen percent of the total losses in the windings. Capacitors should be free of parasitic inductance as their currents change abruptly when the main transistors are turned OFF.

In the modified system, the processes related to the soft-switching of transistors do not affect the motor voltages, unlike in the basic soft-switching system [30]. Fig. 9 shows the current and voltage waveforms of the squirrel-cage induction motor

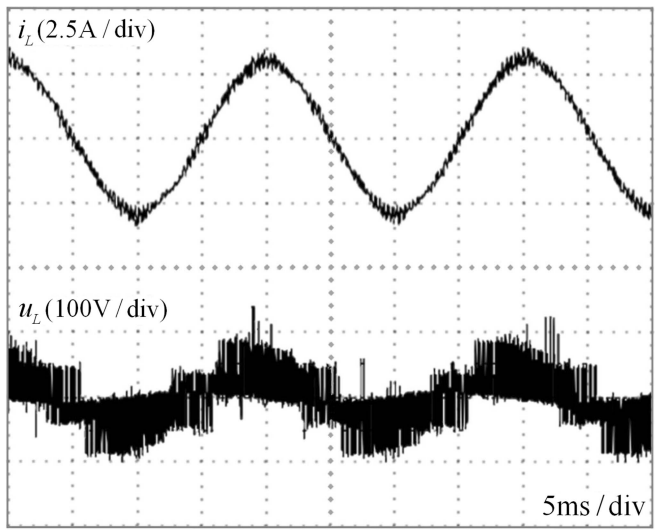

Fig. 9. Oscilloscope view of waveforms of phase current i_L and phase voltage U_L of squirrel-cage induction motor in a basic soft-switching system [30]; $C = 0.5$ μF, $L_a = L_b = 100$ μH, and switching frequency 3 kHz.

recorded in the basic system over two periods. The waveforms of the phase-to-phase voltage, phase voltage, phase current of the induction motor, and the current of the main transistor T1 in the modified soft-switching system are shown in Fig. 10. Analogous waveforms are depicted in Fig. 11 during the regenerative braking of the induction motor.

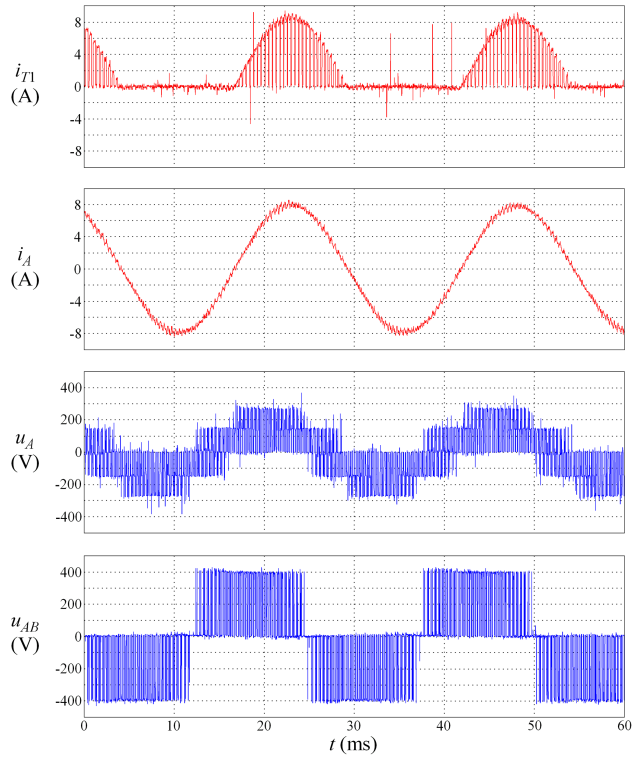

Fig. 10. Waveforms in two output-voltage periods while the motor was supplied: i_{T1}—current of transistor T1; i_A and u_A—phase current and voltage of induction motor, respectively; and u_{AB}—phase-to-phase output voltage of the inverter.

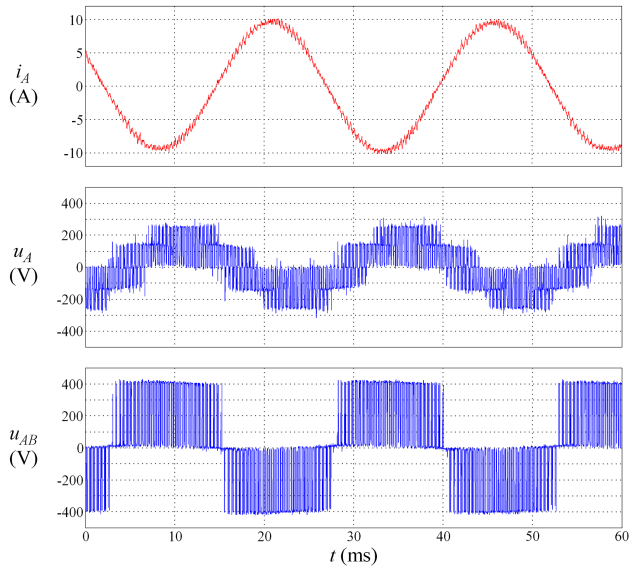

Fig. 11. Waveforms in two output-voltage periods while the motor was braked to provide energy to DC voltage source: i_A and u_A—phase current and voltage of induction motor, respectively; and u_{AB}—phase-to-phase output voltage of the inverter.

The measurements showed that all transistors of the inverter with the modified system were softly switched, and the switching processes did not affect the current waveforms of the load.

V. Power Losses in Inverter With Modified Soft-Switching System

A. Numerical Calculations

The total losses of the inverter with the modified soft-switching system were estimated using numerical calculations performed with the PSpice simulation program and the IGBT model described in [34]. The numerical model of the VSI with soft-switching was validated by comparing selected calculated waveforms with analogous measured waveforms under various operating conditions [30].

Similar to the basic system, the modified soft-switching system is intended for medium- and high-rated-power inverters. Power losses were estimated for two inverters with rated powers of 100 kW (120 A, 600 V) and 1 MW (1200 A, 1 kV). For the 100-kW inverter, IGBTs rated at 3.3 kV and 450 A (SKM450GB33F) and diodes rated at 3.5 kV, 720 A, with a forward voltage of 1.9 V at 450 A (D721S) were used. For the 1 MW inverter, transistors rated at 4.5 kV and 1500 A (CM1500HC-90XA) and diodes rated at 4.5 kV, 1970 A, with a forward voltage of 2.8 V at 1.5 kA (5SDF 20L45) were used (see Table II). The transistors and diodes were selected with some margin to ensure safety in the event of potential increases in voltage or current.

TABLE II
Parameters of IGBTs

Transistor type	V_{CC} (V)	I_C (A)	t_{on} (μs)	t_r (μs)	t_{off} (μs)	t_f (μs)	t_{rr} (μs)	I_{rrm} (A)	V_{CE} (V)
SKM450GB33F	3300	450	0.44	0.12	1.47	0.29	1.49	493	2.86
CM1500HC-90XA	4500	1500	0.80	0.25	7.70	0.50	1.60	2100	2.80
CM300DY-34A	1700	300	0.80	0.20	1.20	0.35	0.45	300	2.45
FZ1500R33HE3	3300	1500	0.76	0.38	3.55	0.35	1.73	1850	3.15

The power losses in the inverter with the modified soft-switching system were compared to those in the inverter using the hard-switching technique. In this comparison, the IGBTs used in the hard-switching inverters had a lower rated voltage and a lower conduction voltage drop than those used in the soft-switching inverters. Power losses in the hard-switching inverter with a rated power of 100 kW were determined using the CM300DY-34A, whereas those for the 1-MW inverter were determined using the FZ1500R33HE3 (see Table II).

The 100-kW and 1-MW inverters were assumed to supply the Y2-315L1-6 squirrel-cage induction motor ($P_N = 110$ kW, $U_N = 400$ V, $I_N = 196$ A) and the Y2-500L2-6 motor ($P_N = 1$ MW, $U_N = 690$ V, $I_N = 1002$ A), respectively. The equivalent circuit of the squirrel-cage induction motor presented in [35] was used. Numerical calculations were performed for three switching frequencies. The parameters of the inductors and capacitors for the assumed values of the coefficient $k_{\max}$ are listed in Table III. Power losses were estimated under the assumption that, during the turn-ON process, the transistor current $I_{T\mathrm{on}}$ does not exceed 10% of the maximum load current $I_{A\max}$, and during the turn-OFF process, the transistor voltage $U_{C\mathrm{off}}$ does not exceed 10% of the source voltage U_{DC}. Therefore, the capacitance C and inductances L_a and L_b were determined according to the following specifications: 100 kW: $I_{A\max} =$

TABLE III
VALUES OF INDUCTANCES AND CAPACITANCE FOR MODIFIED SOFT-SWITCHING SYSTEM

	100 kW			1 MW		
$k_{\max}$	1.5	2.0	2.5	1.5	2.0	2.5
L_a (μH)	4.6	12.6	18.4	4.8	14.4	18.5
R_a (mΩ)	2.20	3.25	4.59	0.29	0.49	0.54
L_b (μH)	1.3	5.3	11.8	1.2	4.8	10.8
R_b (mΩ)	0.99	1.99	2.98	0.14	0.27	0.40
C (μF)	1.6	1.6	1.6	5.2	5.2	5.2

TABLE IV
PARAMETERS OF REPLACEMENT IGBTS

Transistor type	V_{CC} (V)	I_C (A)	t_r (μs)	t_f (μs)	V_{CE} (V)
5SNA 1300K450300 (ABB)	4500	1300	0.60	0.68	3.40
FZ1500R45KL3_B5 (INFINEON)	4500	1500	0.23	1.97	3.25
DIM1200ASM45-TS000 (DYNEX)	4500	1200	0.16	0.53	3.20

332 A, $U_{C\text{off}} = 60$ V, $U_{\text{DC}} = 600$ V, $I_{T\text{on}} = 33.2$ A; 1 MW: $I_{A\max} = 1410$ A, $U_{C\text{off}} = 135$ V, $U_{\text{DC}} = 1350$ V, $I_{T\text{on}} = 141$ A.

When selecting IGBTs other than those listed in Table III, attention should be paid to the conduction voltage drop V_{CE}, current rise time t_r, and current fall time t_f (see Table IV) as these parameters significantly impact conduction and switching losses. Notably, there are significant differences in both the rise and fall times of the transistor currents.

The selected waveforms for the currents and voltages calculated for the 1 MW inverter are presented in Figs. 12 and 13, respectively. In the numerical calculations, the control of transistor T2 was assumed to be disabled when transistor T1 was switched, as explained in Section II-C. Notably, when the motor operated as a generator, the phase shift between the voltage and phase current was significantly greater compared to when energy was supplied to the motor.

The changes in voltages and currents depend not only on the inverter's operating parameters but also on the load. Fig. 14 shows the waveforms when the load torque changes suddenly. It was assumed that during the time interval from 0.2 to 0.4 ms, the load torque was zero, and the VSI supplied only reactive power to the motor. To clarify the presented waveforms, the moment of inertia was reduced several times.

As described in Section II, when transistor T1 is not conducting, a certain current may flow through inductor L1b during stage t_3–t_4 [see Figs. 3 and 4(d)] if the mutual inductance M is smaller than the inductance L_b. Consequently, the next turn-ON process for transistor T1 will not be completely soft. However, if $M = L_b$, then during the conduction of transistor T1 in stage t_5–t_6, where the resonant discharge of capacitor C1 occurs, a small current flows through circuit L1b, diode D1p, and transistor T1 [see Fig. 4(f)]. The maximum value of this current primarily depends on M. While this current can be limited by reducing M relative to L_b, the current in inductor L1b during stage t_3–t_4 is not zero.

The influence of mutual inductance M on the changes in the current of inductor L1b and diode D1p can be expressed as a direct function of M. Since the inductance L_b can vary from

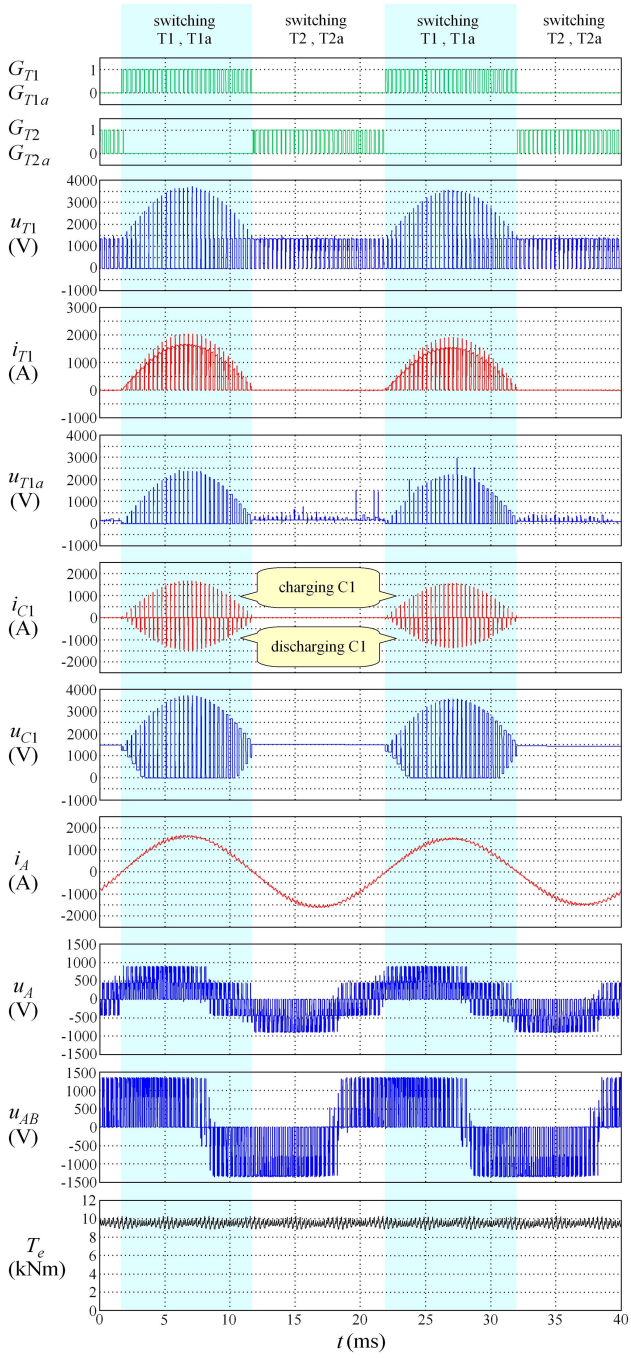

Fig. 12. Waveforms in two output-voltage periods while 1-MW induction motor was supplied; i_A and u_A—phase current and phase voltage of induction motor, respectively; u_{AB}—phase-to-phase voltage; and T_e—electromagnetic torque.

1.2 μH ($k_{\max} = 1.5$) to 11.2 μH ($k_{\max} = 2.5$), it is clearer if the changes in these currents are presented as a function of the parameter k_M:

$$k_M = \frac{|M|}{\sqrt{L_a L_b}}. \tag{24}$$

Fig. 15 shows the relative values of the current I_{L1b} and the relative maximum current value $I_{D1p\max}$ of diode D1p with respect to the maximum current value $I_{A\max}$ of the load as a

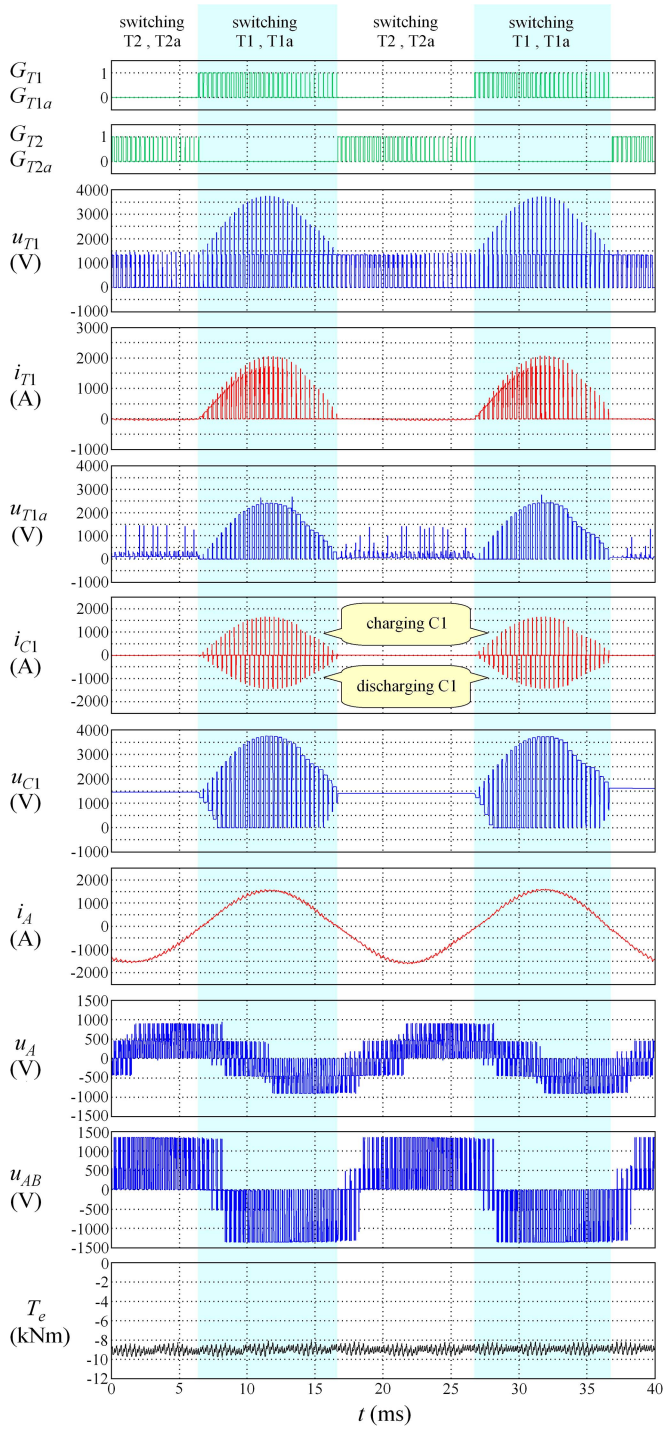

Fig. 13. Waveforms in two output-voltage periods while 1-MW induction motor worked as a generator; waveform markings as in Fig. 12.

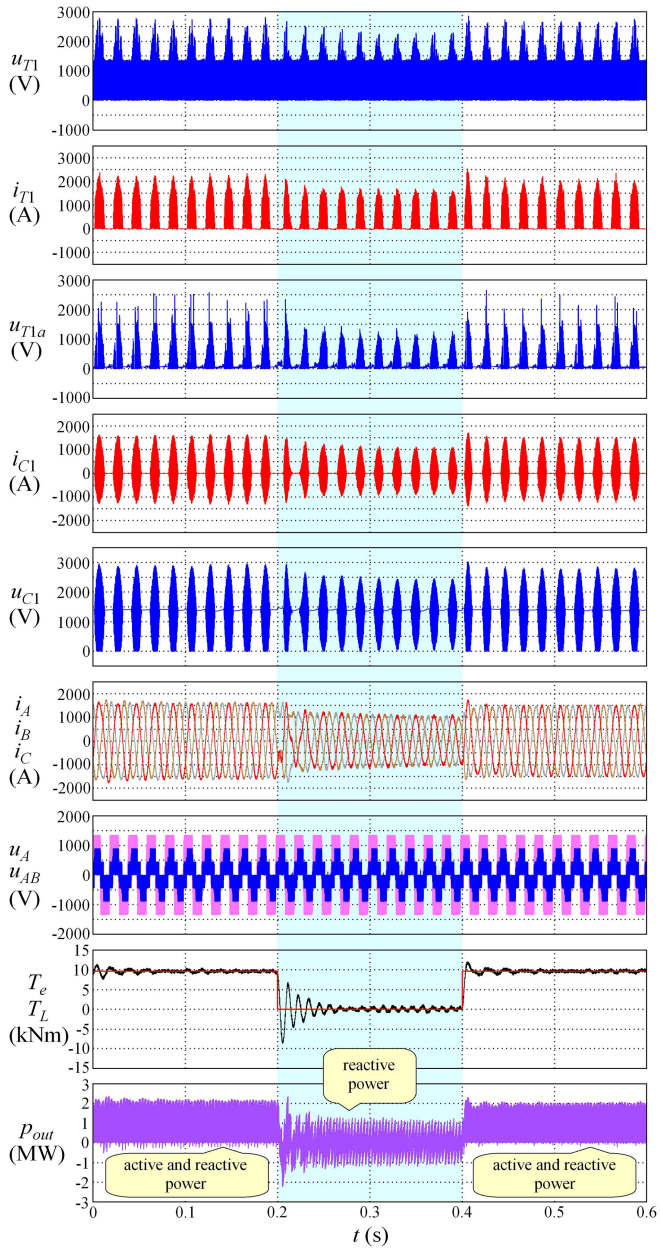

Fig. 14. Waveforms when load torque changed suddenly. T_L—load torque and p_{out}—output power of VSI.

function of k_M. For the given mutual inductance M and the assumed values of $k_{\max}$, and the inductances L_a and L_b, the current in inductor L1b during the time interval t_3-t_4 and the maximum current in diode D1p during period t_5–t_6 can be estimated.

The relative current values for the condition $M = L_b$ are indicated for $k_{\max} = 1.5$, 2.0, and 2.5, where $k_{\max}$ is the ratio of the maximum capacitor voltage to the supply voltage U_{DC}. The effect of changes in mutual inductance M on the waveforms of the inverter with the modified soft-switching system is shown in Fig. 16. The current and voltage waveforms of the 1-MW inverter, calculated for M differing from L_b by $\pm 20\%$, were compared with the analogous waveforms for $M = L_b$.

B. Estimation of Power Losses

Power losses were calculated separately for each inverter element as the integral of the product of the current and voltage of the element in question. Unlike VSIs operating with a hard-switching technique, diodes in soft-switching systems do not generate turn-OFF losses. However, power losses do occur

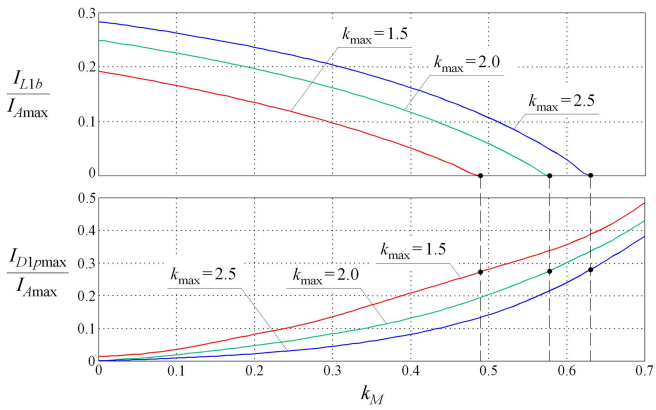

Fig. 15. Relative value of (a) current I_{L1b} and (b) maximum current value $I_{D1p\max}$ with respect to maximum load current $I_{A\max}$ as a function of k_M.

TABLE V
POWER LOSSES OF 100-KW INVERTER WITH MODIFIED SOFT-SWITCHING SYSTEM

f_n (Hz)	$k_{\max}=1.5$	$k_{\max}=2.0$	$k_{\max}=2.5$	hard switching
Total switching losses (W)				
1000	328	165	109	372
2000	601	279	169	773
4500	1245	516	318	1742
Conduction losses in transistors and diodes (W)				
1000	1269	1301	1322	1297
2000	1289	1333	1360	1296
4500	1329	1386	1438	1295
Conduction losses in inductors (W)				
1000	125	252	377	---
2000	125	251	388	---
4500	127	243	416	---
Total losses of the inverter (W)				
1000	1722	1718	1808	1669
2000	2015	1863	1916	2070
4500	2701	2146	2172	3037
Efficiency (%)				
1000	98.31	98.31	98.23	98.40
2000	98.02	98.17	98.12	97.98
4500	97.37	97.90	97.87	97.05

in additional components of soft-switching circuits, such as auxiliary transistors, their freewheeling diodes, and inductors, which must be considered when estimating total power losses. The IGBT model described in [34] was used in the estimation of power losses. This model allows one to consider the nonlinear properties of the IGBTs, the variable values of the transistor, the diode-conduction voltage drops, and the switching processes without having to linearize the current and voltage waveforms, as in the case of analytical calculations.

The turn-ON losses of these transistors were nearly zero due to the resonance of the capacitor discharge current. Power losses in the inductors depend on their internal resistance, conduction times, and currents. The total power losses for the inverters considered are listed in Table V (100 kW) and Table VI (1 MW) for three values of $k_{\max}$.

The estimation of power losses and efficiency for a 100-kW VSI is comparable to that of an inverter with a rated power

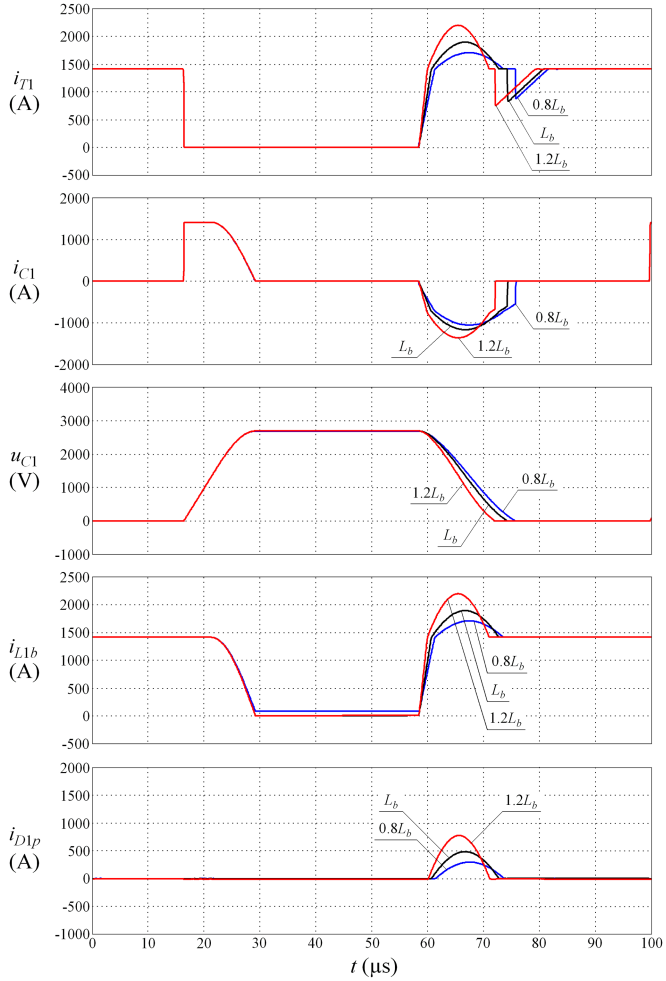

Fig. 16. Current and voltage waveforms of 1-MW inverter calculated for $M = 0.8L_b$, $M = L_b$, and $M = 1.2L_b$.

TABLE VI
POWER LOSSES OF 1-MW INVERTER WITH MODIFIED SOFT-SWITCHING SYSTEM

f_n (Hz)	$k_{\max}=1.5$	$k_{\max}=2.0$	$k_{\max}=2.5$	hard switching
Total switching losses (W)				
1000	2716	1074	708	10382
2000	5184	1841	1086	20950
4500	10860	3744	2370	47274
Conduction losses in transistors and diodes (W)				
1000	6278	6455	6607	5990
2000	6412	6673	6867	5986
4500	6693	7173	7514	5976
Conduction losses in inductors (W)				
1000	329	666	1029	---
2000	333	688	1077	---
4500	346	744	1203	---
Total losses of the inverter (W)				
1000	9322	8195	8345	16372
2000	11929	9202	9030	26935
4500	17899	11661	11087	53251
Efficiency (%)				
1000	99.08	99.19	99.17	98.39
2000	98.82	99.09	99.11	97.38
4500	98.24	98.85	98.90	94.94

10 times higher. Inverters with several hundred kilowatts are currently based on SiC MOSFETs. However, the reduction in switching losses was qualitatively similar to that observed in VSIs based on IGBTs.

Power losses in VSIs with the soft-switching system were compared with those in a VSI using a hard-switching technique. Notably, due to their higher operating voltage, IGBTs with a higher rated voltage drop must be used in inverters with a soft-switching system, unlike IGBTs with lower voltage drops used in hard-switching systems.

Notably, the diodes are turned OFF without any loss, and their currents drop to zero when their operating state changes. For diodes D1s and D2s (at time t_4) in the considered phase, the current is relatively low, and no abrupt reverse recovery current occurs, unlike in VSIs using hard-switching techniques.

Although power losses in the inductor windings amount to approximately 12% of the total losses in extreme cases, the efficiency of the inverter with the soft-switching system is significantly higher compared to the VSI with hard-switching IGBTs. As mentioned earlier, these losses can be further reduced by using inductors with ferrite cores. Notably, even for $k_{\max} = 1.5$, the efficiency of the VSI with the proposed soft-switching system was higher than that of the inverter with the hard-switching technique.

Fig. 17 illustrates the relationship between total switching losses on the switching frequency and the coefficient $k_{\max}$ for both inverters. Fig. 18 compares the losses in the inverter with the modified soft-switching system to those in the inverter with the hard-switching system. Fig. 19 compares the efficiencies of the inverter with the modified soft-switching system to those of the inverter with the hard-switching technique.

The efficiency of a 100-kW inverter with a hard-switching system is slightly higher than that of an inverter with a soft-switching system, albeit only at a switching frequency of 1 kHz. In other cases, when the modified soft-switching system is used, the efficiency of the inverters with soft switching is higher than that of the inverter with hard switching by approximately 2%.

The difference in efficiency between inverters using different switching techniques increases with switching frequency. Fig. 20 shows the efficiencies of the 1-MW VSI as a function of output load power for a switching frequency of 4.5 kHz. Notably, the efficiency of high-power inverters with the modified soft-switching system exceeded that of inverters using the hard-switching technique, even when $k_{\max}$ was significantly less than 2.0. This should be taken into account when selecting transistors.

The maximum efficiency of the 1-MW VSI with the proposed soft-switching system was approximately 99% at a switching frequency of 4.5 kHz. Inverters with various soft-switching systems, as presented in [19], [20], [22], and [25] achieved efficiencies ranging from 98% to 99%. However, these efficiencies were measured at load powers up to 10 kW and switching frequencies of 20 kHz or 30 kHz. In [26], a soft-switching system with an auxiliary inductor was proposed, achieving an efficiency of approximately 99.6%. However, the authors of this article noted that the use of this system is not recommended because employing only one inductor can prevent the simultaneous use of all three phases, potentially leading to collisions when accessing

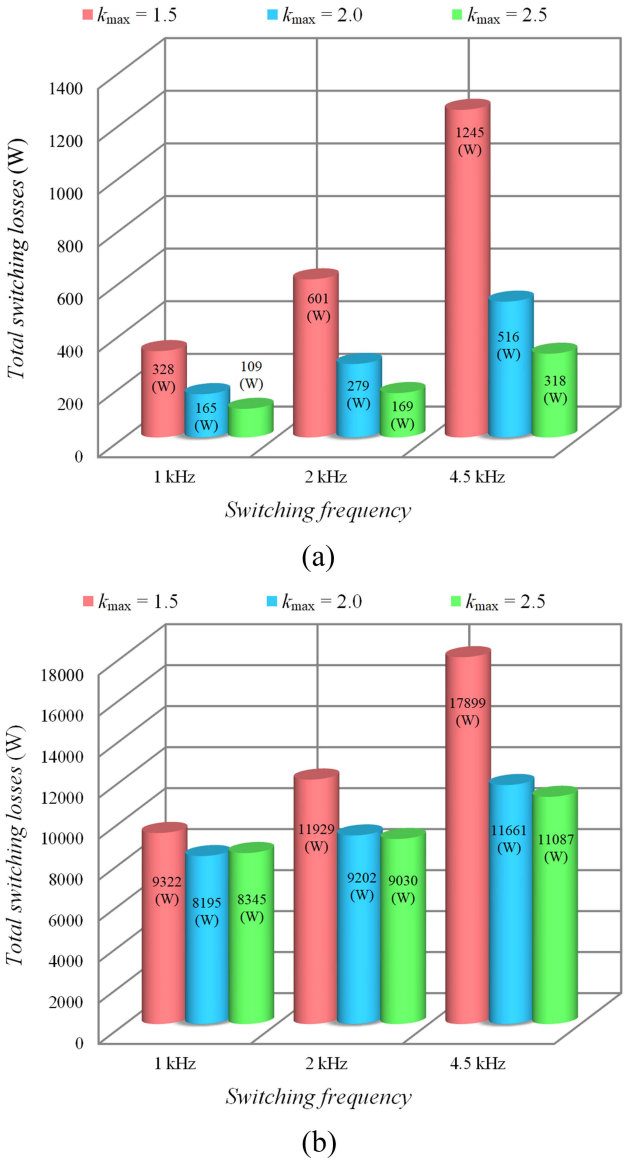

Fig. 17. Total switching losses as functions of switching frequency and coefficient $k_{\max}$ for an inverter with rated power levels of (a) 100 kW and (b) 1 MW.

an auxiliary circuit. Notably, in each soft-switching system discussed in the aforementioned studies, disturbances in the control system may cause abrupt capacitor discharge or interruptions in the current of auxiliary inductors.

To compare the switching techniques, the total harmonic distortion (THD) was estimated for both soft- and hard-switching VSIs (see Table VII). The modulation depth factor was set at 0.85, and the switching frequency was 4.5 kHz.

The results in Table VII indicate that the THD values in the VSI with the modified soft-switching system are similar to those in the VSI with the hard-switching technique.

C. Comparison of VSIs With Soft-Switching Systems

VSIs with soft-switching systems are commonly compared based on the number of additional transistors and passive

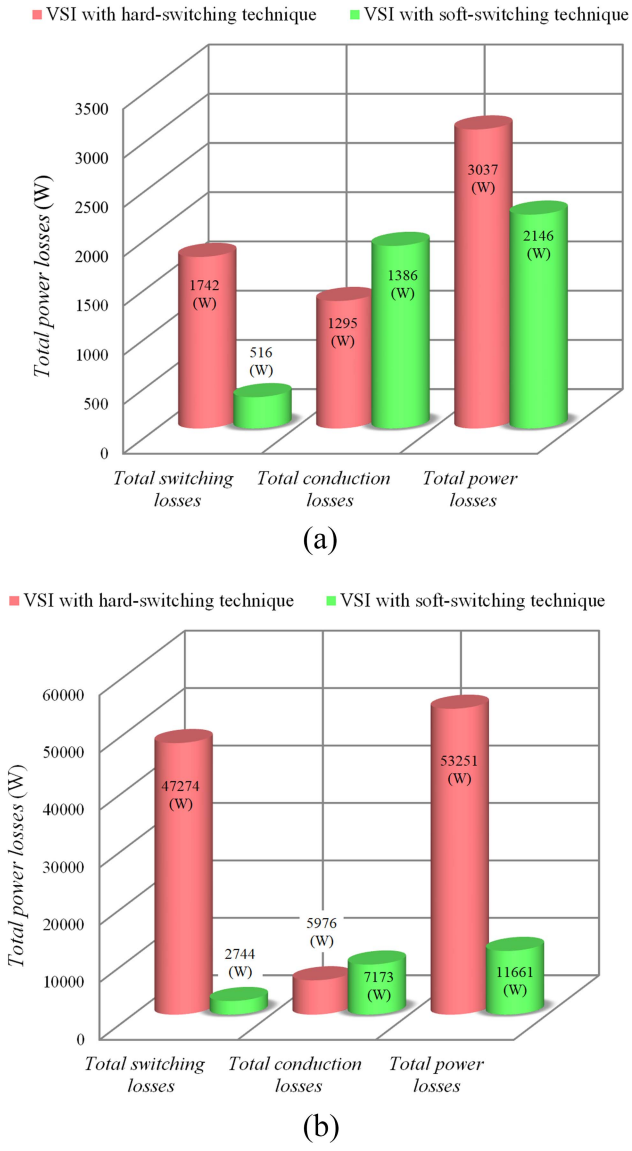

Fig. 18. Comparison of switching losses, conduction losses, and total power losses under a switching frequency of 4.5 kHz for inverters with rated power levels of (a) 100 kW and (b) 1 MW; $k_{\max} = 2.0$.

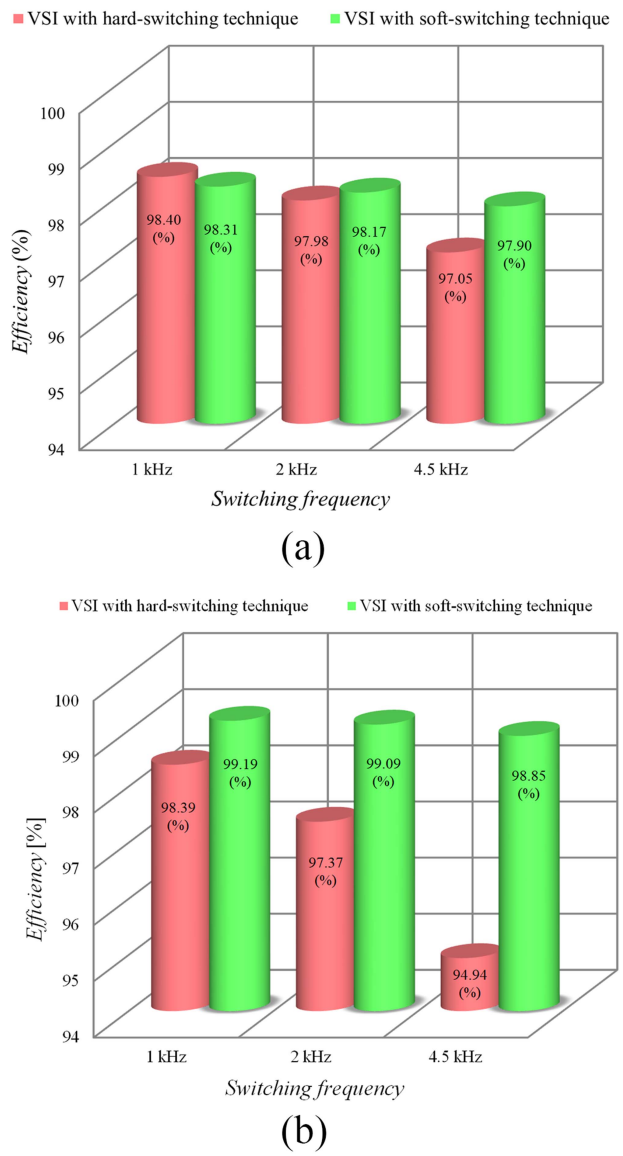

Fig. 19. Efficiency comparison for inverters with rated power levels of (a) 100 kW and (b) 1 MW; $k_{\max} = 2.0$.

TABLE VII
THD VALUES FOR 100 HARMONICS (IN PER CENT)

$k_{\max}$	U_A (THD %)	U_{AB} (THD %)	I_A (THD %)
1.5	40.15	40.21	0.85
2.0	40.12	40.05	0.86
2.5	41.96	41.95	1.01
hard switching	40.23	40.22	0.85

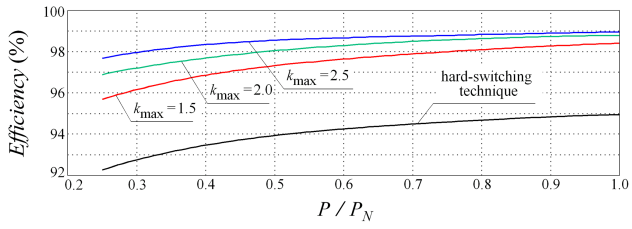

Fig. 20. Efficiency of 1-MW VSI as a function of normalized output load power P/P_N for three values of parameter $k_{\max}$ and for VSI with hard-switching technique.

components, as well as their efficiency. However, efficiency can vary significantly depending on factors such as load power, switching frequency, and the type of semiconductor used. It is important to note that many comparisons do not account for factors like the complexity of the control system or the VSI's resistance to disturbances that could potentially damage the inverter. The number of additional components becomes more relevant when producing VSIs in large quantities, such as inverters for energy conversion from renewable sources. In contrast, for inverters with a rated power of several hundred kW or several MW, used in industrial applications like mining,

TABLE VIII
COMPARISON OF NUMBER OF ADDITIONAL COMPONENTS

Additional components	[19]	[20]	[22]	[25]	[26]	This article
Auxiliary transistors	6	6	6	-	6	6
Capacitors	3+6*	6	6+6*	3	2	6
Inductors	3	3	12**	3+6**	1	12**
Efficiency (%)	98.6	98.3	98.8	98.7	99.6	98.6

* including capacitors connected in parallel to the main transistors
** including the number of coupled inductors

TABLE IX
COMMENTS ON VSIS WITH SOFT SWITCHING

	Comments	References
1.	A risk of sudden capacitor discharge through main transistors in case of disturbances	[19], [20], [22], [26]
2.	The auxiliary transistors must be turned ON before switching the main transistors	[19], [20], [22]
3.	Employing only one inductor can prevent the simultaneous use of all three phases, potentially leading to collisions	[26]
4	The switching frequency must be updated at the beginning of each switching cycle. Rather for photovoltaic systems, not for vector control of squirrel-cage induction motor.	[25]

metallurgy, and electric traction, the reliability of operation is of paramount importance, whereas the number of additional components may be of secondary concern. Table VIII presents a comparison of the number of additional components and the efficiencies of several proposed soft-switching systems.

Comments on the control of inverters with individual soft-switching systems and their resistance to disturbances are presented in Table IX.

When selecting a soft-switching system for a VSI, it is important to consider the number of additional components, the risk of emergency states, and the operational reliability of the VSI, especially at high power ratings. Additionally, the complexity of the control system and the dimensions of the VSI with the chosen soft-switching system should be taken into account. The cost of the device is also significantly influenced by the quantity produced.

VI. SUMMARY

A. Conclusion

Similar to the basic soft-switching system in a three-phase VSI, the modified system does not connect capacitors in parallel with the main transistors or inductors in series with the auxiliary transistors. Consequently, the capacitor discharges through the main transistors, and abrupt interruptions in the inductor currents are eliminated.

The modified soft-switching system offers several advantages over its basic counterpart. The soft-switching processes do not affect the shape of the phase-to-phase voltage or the phase voltage of the load, which is crucial for protecting the induction motor's windings and insulation from exceeding their rated voltage. Additionally, the control system is significantly simplified because the auxiliary transistors are controlled by the same signal as the main transistors, enhancing the reliability of VSIs operating with the modified soft-switching system.

Laboratory tests confirmed that both the main and auxiliary transistors switched softly, significantly reducing switching losses and improving the efficiency of the voltage inverter, despite additional conduction losses in the auxiliary transistors, diodes, and inductors. However, like all soft-switching systems, the modified system has limitations concerning control parameters, such as switching frequency and maximum amplitude-modulation ratio.

The presence of capacitors in the proposed soft-switching system protects all transistors from overvoltage. Additionally, the inductors placed between the main transistors and load clamps limit the rate of increase in short-circuit current if both main transistors are accidentally turned ON in a given phase. It is important to note that the control algorithm for the main transistors can remain the same as that used in VSIs with typical PWM or vector control methods.

The proposed soft-switching system is recommended not only for high-power VSIs used in industrial drive systems, electric traction, and energy conversion systems but also for lower-power inverters, particularly those used in renewable energy applications.

B. Future Works

Future research should focus on analyzing the efficiency of the VSI with the proposed soft-switching system using different IGBTs. This is important because the parameters of IGBTs with the same rated voltage and current can vary significantly, particularly regarding current rise and fall times during switching processes.

Vector control is commonly used in drives for induction motors with rated powers exceeding several kilowatts. Therefore, it is essential to investigate the interaction between the inverter and the induction motor, as resonance processes may influence the conduction times of the main transistors. This issue is also significant for VSIs used in renewable energy systems.

It is important to note that using SiC MOSFETs in VSIs does not completely resolve the problem of switching losses. Although SiC elements have shorter switching times compared to IGBTs, they operate at higher switching frequencies. Thus, the challenge of reducing switching losses remains pertinent and will continue to be a relevant issue.

REFERENCES

[1] G. Feix, S. Dieckerhoff, J. Allmeling, and J. Schonberger, "Simple methods to calculate IGBT and diode conduction and switching losses," in *Proc. 13th Eur. Conf. Power Electron. Appl.*, 2009, pp. 1–8.
[2] A. D. Rajapakse, A. M. Gole, and P. L. Wilson, "Approximate loss formulae for estimation of IGBT switching losses through EMTP-type simulations," in *Proc. Int. Conf. Power Syst. Transients*, 2005, pp. 1–6.
[3] A. K. Sadigh, V. Dargahi, and K. A. Corzine, "Investigation of conduction and switching power losses in modified stacked multicell converters," *IEEE Trans. Ind. Electron.*, vol. 63, no. 12, pp. 7780–7791, Dec. 2016, doi: 10.1109/TIE.2016.2607160.
[4] O. Oñederra, I. Kortabarria, I. Martínez de Alegría, J. Andreu, and J. I. Gárate, "Three-phase VSI optimal switching loss reduction using variable switching frequency," *IEEE Trans. Power Electron.*, vol. 32, no. 8, pp. 6570–6576, Aug. 2017, doi: 10.1109/TPEL.2016.2616583.
[5] E. Hiraki, T. Tanaka, and M. Nakaoka, "Zero-voltage and zero-current soft-switching PWM inverter," in *Proc. 36th Eur. Conf. Power Electron. Spec. Conf.*, 2005, pp. 798–803, doi: 10.1109/EPE.2005.219661.

[6] B. Panda, D. P. Bagarty, and S. Behera, "Soft-switching DC-AC converters: - A brief literature review," *Int. J. Eng. Sci. Techn.*, vol. 2, no. 12, pp. 7004–7020, 2010. [Online]. Available: https://www.researchgate.net/publication/50384248_SOFT-SWITCHING_DC-AC_CONVERTERS-_A_BRIEF_LITERATURE_REVIEW

[7] M. R. Amini and H. Farzanehfard, "Three-phase soft-switching inverter with minimum components," *IEEE Trans. Ind. Electron.*, vol. 58, no. 6, pp. 2258–2264, Jun. 2011, doi: 10.1109/TIE.2010.2064280.

[8] R. Li and D. Xu, "A zero-voltage switching three-phase inverter," *IEEE Trans. Power Electron.*, vol. 29, no. 3, pp. 1200–1210, Mar. 2014, doi: 10.1109/TPEL.2013.2260871.

[9] M. Khalilian, A. D. Zadeh, and E. Adib, "New three-phase zero-voltage switching PWM inverter using resonant dc-link," in *Proc. 6th Power Electron. Drive Syst. Technol. Conf.*, 2015, pp. 521–526, doi: 10.1109/PEDSTC.2015.7093329.

[10] A. De and M. Barai, "An improved zero voltage switching SVPWM for three phase inverter," in *Proc. 11th IEEE Int. Conf. Compat., Power Electron. Power Eng.*, 2017, pp. 169–174, doi: 10.1109/CPE.2017.7915164.

[11] K. Mozaffari and M. Amirabadi, "A highly reliable and efficient class of single-stage high-frequency ac-link converters," *IEEE Trans. Power Electron.*, vol. 34, no. 9, pp. 8435–8452, Sep. 2019, doi: 10.1109/TPEL.2018.2888583.

[12] Y. Wu, N. He, and D. Xu, "Generalized space-vector-modulation method for soft-switching three-phase inverters," *IEEE Trans. Power Electron.*, vol. 36, no. 5, pp. 6030–6045, May 2021, doi: 10.1109/TPEL.2020.3026824.

[13] Y. Li, F. C. Lee, and D. Boroyevich, "A three-phase soft-transition inverter with a novel control strategy for zero-current and near zero-voltage switching," *IEEE Trans. Power Electron.*, vol. 16, no. 5, pp. 710–723, Sep. 2001. [Online]. Available: https://ieeexplore.ieee.org/document/949504

[14] B. L. Martinez, R. Li, K. Ma, and D. Xu, "Hard switching and soft switching inverters efficiency evaluation," in *Proc. Int. Conf. Elect. Mach. Syst.*, 2008, pp. 1752–1757. [Online]. Available: https://ieeexplore.ieee.org/document/4771018

[15] R. C. Beltrame, J. R. R. Zientarski, M. L. da Silva Martins, J. R. Pinheiro, and H. L. Hey, "Simplified zero-voltage-transition circuits applied to bidirectional poles: Concept and synthesis methodology," *IEEE Energy Convers. Congr. Expo.*, vol. 26, no. 6, pp. 1765–1776, Jun. 2011, doi: 10.1109/ECCE.2009.5316237.

[16] P. Sun, J. S. Lai, C. Liu, and W. Yu, "A 55-kW three-phase inverter based on hybrid-switch soft-switching modules for high-temperature hybrid electric vehicle drive application," *IEEE Trans. Ind. Appl.*, vol. 48, no. 3, pp. 962–969, May/Jun. 2012. [Online]. Available: https://ieeexplore.ieee.org/document/6170561

[17] C. Galea, "New topology of three phase soft switching inverter using a dual auxiliary circuit," in *Proc. 15th Eur. Conf. Power Electron. Appl.*, 2013, pp. 1–9, doi: 10.1109/EPE.2013.6631812.

[18] A. Pal and K. Basu, "A soft-switched high-frequency link single-stage three-phase inverter for grid integration of utility scale renewables," *IEEE Trans. Power Electron.*, vol. 34, no. 9, pp. 8513–8527, Sep. 2019, doi: 10.1109/TPEL.2018.2889795.

[19] Q. Wang and Y. Wang, "Research on a novel high-efficiency three-phase resonant pole soft-switching inverter," *IEEE Trans. Power Electron.*, vol. 36, no. 5, pp. 5845–5857, May 2021, doi: 10.1109/TPEL.2020.3029186.

[20] E. Chu, J. Song, D. Yang, and H. Zhang, "An auxiliary resonant pole soft-switching inverter with low pre-charge current," *IEEE Trans. Power Electron.*, vol. 38, no. 10, pp. 12780–12800, Oct. 2023, doi: 10.1109/TPEL.2023.3297836.

[21] C. Lei, A. Li, X. Gui, and S. Li, "A novel auxiliary resonant pole soft-switching inverter with simple control," in *Proc. 6th Int. Conf. Electron. Technol.*, 2023, pp. 811–816, doi: 10.1109/ICET58434.2023.10211831.

[22] Q. Wang, L. Li, and Y. Wang, "An efficient zero-voltage switching resonant pole inverter with high reliability," *IEEE Trans. Circuits Syst. II, Exp. Briefs*, vol. 70, no. 1, pp. 156–160, Jan. 2023, doi: 10.1109/TCSII.2022.3196060.

[23] K. Lulbadda, R. D. Seram, N. Shrestha, T. Sidhu, and S. Williamson, "An analysis of advanced soft-switching techniques for dc–ac power converters based on auxiliary circuits," in *Proc. IEEE Int. Conf. Ind. Technol.*, 2023, pp. 1–6, doi: 10.1109/ICIT58465.2023.10143173.

[24] H. Lu, Q. Wang, J. Chai, and Y. Li, "Review of three-phase soft switching inverters and challenges for motor drives," *CES Trans. Elect. Mach. Syst.*, vol. 8, no. 2, pp. 177–190, Jun. 2024, doi: 10.30941/CESTEMS.2024.00030.

[25] S. Bagawade, M. Pahlevani, and P. Jain, "Novel soft-switched three-phase inverter with output current ripple cancellation," *IEEE Trans. Power Electron.*, vol. 38, no. 1, pp. 1232–1248, Jan. 2023, doi: 10.1109/TPEL.2022.3203055.

[26] T. Lehmeier, A. Amler, Y. Zhou, and M. März, "Three-phase ARCP inverter using soft-switching with a single shared inductor," *IEEE Trans. Power. Electron.*, vol. 39, no. 2, pp. 2505–2521, Feb. 2024, doi: 10.1109/TPEL.2023.3325162.

[27] S. Li, M. Yang, T. Song, J. Long, and Y. Ma, and D. Xu, "A simple structure of auxiliary resonant commutated pole SiC-based Soft-switching inverter," *IEEE Trans. Transp. Electrific.*, to be published, doi: 10.1109/TTE.2024.3403156.

[28] Q. Wang, J. He, Y. Wang, and H. Bai, "An efficient three-phase soft-switching inverter with simplified asymmetric single auxiliary circuit on each bridge arm for low-speed ac motor drive," *IEEE Trans. Circuits Syst. I, Reg. Papers*, vol. 71, no. 9, pp. 4388–4399, Sep. 2024, doi: 10.1109/TCSI.2024.3418432.

[29] W. Mazgaj, B. Rozegnał, and Z. Szular, "Proposal of a new soft switching system for three-phase voltage source inverters," in *Proc. 19th Eur. Conf. Power Electron. Appl.*, 2017, pp. P.1–P.10, doi: 10.23919/EPE17ECCEEurope.2017.8098936.

[30] W. Mazgaj, Z. Szular, and B. Rozegnał, "Soft-switching system with safe connections of capacitors and inductors in three-phase two-level voltage source inverter," *IEEE Trans. Power Electron.*, vol. 36, no. 6, pp. 6443–6456, Jun. 2021, doi: 10.1109/TPEL.2020.3036171.

[31] Y. Yang, "A passive augmented circuit for EMI reductions of full-bridge inverters with conventional phase shift control in wireless power transfer systems," *IEEE Trans. Power Electron.*, vol. 38, no. 11, pp. 13286–13297, Nov. 2023, doi: 10.1109/TPEL.2023.3300915.

[32] E. Chu, Z. Wang, and Y. Kang, "Analysis and implementation of passive soft switching snubber for PWM inverters," *J. Power Electron.*, vol. 23, pp. 48–57, 2023, doi: 10.1007/s43236-022-00520-z.

[33] B. Rozegnał, Z. Szular, and W. Mazgaj, "Modifications of the soft switching system resistant to disturbances in control systems of voltage sources inverters," *Tech. Trans.*, vol. 115, pp. 141–155, 2018, doi: 10.4467/2353737XCT.18.152.9100.

[34] F. Chimento, N. Mora, M. Bellini, I. Stevanovic, and S. Tomarchio, "A simplified spice based IGBT model for power electronics modules evaluation," in *Proc. 37th Annu. Conf. IEEE Ind. Electron. Soc.*, 2011, pp. 1155–1160, doi: 10.1109/IECON.2011.6119471.

[35] D. Cholewa, W. Mazgaj, and Z. Szular, "Cooperation between vector controlled cage induction motor and voltage source inverter operating with soft switching system," in *Proc. 54th Int. Symp. Elect. Mach.*, 2018, pp. 1–5, doi: 10.1109/ISEM.2018.8442764.

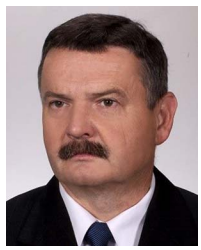

Witold Mazgaj received the Ph.D. degree in electrical engineering from the University of Mining and Metallurgy, Cracow, Poland, in 1986, and the D.Sc. degree in electrical engineering from the Poznan University of Technology, Poznań, Poland, in 2012.

Since 1978, he has been with the Faculty of Electrical and Computer Engineering, Cracow University of Technology, Cracow, Poland. He is the author or coauthor of about 120 papers and 10 patents. His research interests include soft-switching systems of power electronics converters and electromagnetic phenomena in nonlinear circuits.

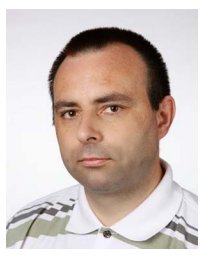

Zbigniew Szular received the Ph.D. degree in electrical engineering from the Cracow University of Technology, Cracow, Poland, in 2011.

Since 2012, he has been with the Faculty of Electrical and Computer Engineering, Cracow University of Technology. He is the author or coauthor of about 35 papers and 5 patents. His research interests include the designing of electrical installations on each voltage level and electrical power systems and power electronics, including electromagnetic phenomena.